We are IntechOpen, the world's leading publisher of Open Access books
Built by scientists, for scientists

6,900
Open access books available

186,000
International authors and editors

200M
Downloads

Our authors are among the

154
Countries delivered to

TOP 1%
most cited scientists

12.2%
Contributors from top 500 universities

CLARIVATE ANALYTICS
BOOK CITATION INDEX
INDEXED

WEB OF SCIENCE™

Selection of our books indexed in the Book Citation Index in Web of Science™ Core Collection (BKCI)

Interested in publishing with us?
Contact book.department@intechopen.com

Numbers displayed above are based on latest data collected.
For more information visit www.intechopen.com

7

Optimization and Simulation for Ceramic Injection Mould of ZrO_2 Fiber Ferrule

Bin Lin, Meiming Zhang, Chuhan Wu and Feng Liu
Tianjin University, China

1. Introduction

Fiber ferrule is a crucial part for manufacturing fiber connectors. It is fairly difficult to produce fiber ferrule because that it requires high dimension accuracy. Currently, YTZ ceramic powder is the main material used to produce fiber ferrule and Ceramic Injection Molding (CIM) is a new fabricating method capable of producing ZrO_2 fiber ferrule (Fig. 1(a), Fig. 1(b)) with complex geometry and high accuracy. ZrO_2 fiber ferrule quality is significantly influenced by the process conditions of CIM. Therefore, the main focus of this paper is to optimize mould structure and processing parameters based on the simulation of CIM, which promotes solid load of ceramic powder and product quality. Optimal process conditions of Ceramic Injection Molding could be determined by analyzing the simulation results. It has been found that runner cross-section shape and runner system contribute to the efficiency and filling process significantly. Hence, optimal runner cross-section shape and runner system are proposed. Reducing the gravity influence on CIM is also suggested. Moreover, optimization of cooling system could be considered an effective way to improve the dimensional precision and surface quality of ZrO_2 fiber ferrule.

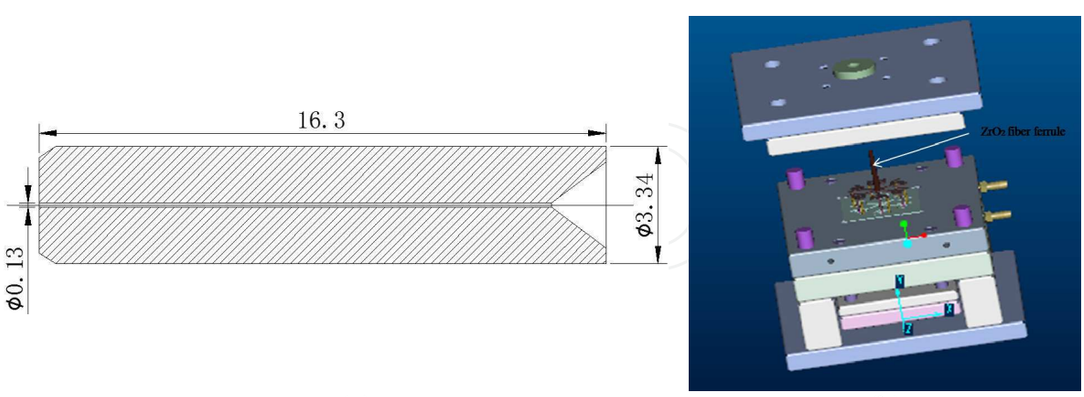

(a) (b)

Fig. 1. ZrO_2 fiber ferrule; (a) Roughcast of the ZrO_2 fiber ferrule; (b) Geometry of the mould.

2. Optimization of runner cross-section shape

During filling stage, the melt is firstly injected into mould cavity and this stage is accomplished as the mould cavity is fully filled by melt. Therefore, it is of great importance

to control melt flow pattern within mould cavity, which could promote the solid load of ceramic powder. Cooling time and many product defects like cavitations, weld line, short shot and product deformation are related to the melt flow pattern. The melt flow pattern is influenced by many factors like the dimension of runner cross-section shape and runner system arrangement. Hence, optimized runner cross-section shape and well-designed runner system would be beneficial to the Ceramic Injection Molding. In order to investigate the melt flow pattern, pressure changes, temperature, cavitations etc., we use Moldflow Plastic Insight (MPI) to simulate the melt flow pattern within the mould cavity. Also, potential defects would be predicted during this simulation. The optimal runner cross-section shape could be determined though analyzing simulation results of different runner cross-section shapes.

Runners should ensure that the melt ejected from injection machine can smoothly flow through runners and fully fill mould cavity. What is more, runners should adequately transfer pressure to all the positions of mould cavity to obtain high quality products during filling process.

Common runner cross-section shapes (Fig. 2) are circular, ladder, U-shape (combination of circular and ladder), semicircular and rectangular. It usually is recommended to use the first three runner cross-section shapes. Considering the ratio of volume to its surface area, circular cross-section shape is most suitable, with minimal pressure drop and heat loss. However, templates on both sides of circular runners need to be processed, which causes much higher cost. Furthermore, semicircles on both surfaces of those two templates of circular runners have to be aligned accurately.

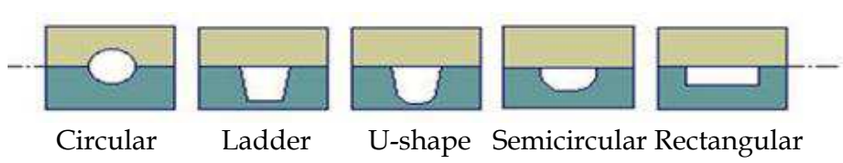

Fig. 2. Common runner cross-section shapes.

Ladder runner cross-section shape requires one processed template only, which still works well. Ladder runner is commonly used in three-plate mould. Circular runner cross-section shape is rarely adopted in three-plate mould for it may be difficult to demould and cause interference between runner and sliding part of templates. Different runner cross-section shapes could be compared by hydraulic diameter (Table 1) which is the index of flow resistance. The larger the hydraulic diameter is, the lower the flow resistance is. The definition of hydraulic diameter is described as equation 1.

$$D_h = \frac{4A}{P} \tag{1}$$

Where D_h is the hydraulic diameter, A is the section area and P is the perimeter.

Equivalent hydraulic diameters of various runner cross-section shapes are compared in Table 2.

Cross-section	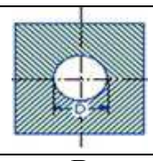	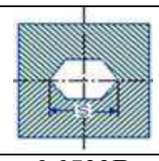	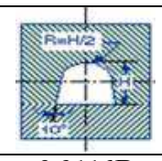	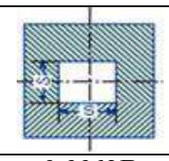
D_h	D	$0.9523D$	$0.9116D$	$0.8862D$
Cross-section	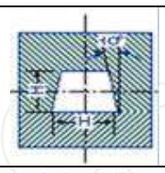	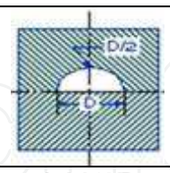	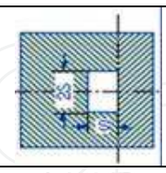	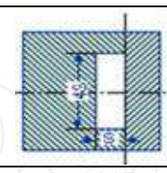
D_h	$0.8711D$	$0.8642D$	$0.8536D$	$0.7090D$

Table 1. Equivalent hydraulic diameters of various runner cross-section shapes.

	Cross-section Shapes	Equivalent Diameters
A	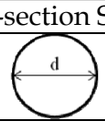	d
B	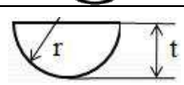	$2\sqrt{\frac{r^2\cos^{-1}x - r(r-t)\sin(\cos^{-1}x)}{\pi}} \quad x = \frac{r-t}{r}$
C	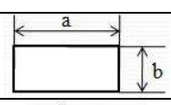	$2\sqrt{\frac{ab}{\pi}}$
D	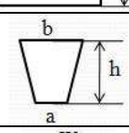	$\sqrt{\frac{2(a+b)h}{\pi}}$
E	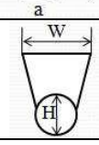	$\sqrt{\frac{2H}{\pi}}\sqrt{(W + H\arctan(\frac{H}{W}))}$

Table 2. Comparison between equivalent diameters of various runner cross-section shapes.

2.1 Analytical solutions of various runner cross-section shapes

The main factors influencing melt flow are injection pressure, melt temperature and viscosity, mould temperature, runner cross-section area and geometric cross-section shape. The geometric cross-section shape determines runner efficiency.

It requires the following conditions to improve runner efficiency (Pan et al., 1995). Runner resistance to the melt flow, which is normally caused by the friction between melt and inner runner surface, should be as low as possible to ensure that the melt can fully fill the mould cavity before solidifying.

The heat loss should be minimal as the melt flows through runner. When the melt with high temperature flows through runner with comparatively lower temperature, melt would transfer its heat to the mould, which increases mould temperature. On the other hand, the melt temperature decreases. Also, melt viscosity increases when melt temperature becomes lower, which makes melt fluidity worse. When the temperature decreases to a certain degree, temperature distribution within inner side of melt becomes significantly inhomogeneous that causes many defects in the products. In this case, we can improve the

injection pressure moderately. However, it would affect clamp if injection pressure becomes too high.

For improving runner efficiency, many measurements could be adopted during designing and manufacturing stages. Firstly, the area of runner cross-section shape can be increased, which decreases the resistance to melt flow. However, it would waste energy and raw materials if the area of runner cross-section shape becomes oversize. Secondly, the contact area between runner and melt could be diminished by decreasing periphery length of runner cross-section shape. Thirdly, runner layout should be simple and its length should be minimal. Finally, the runner surface roughness can be decreased. Normally, R_a is between 0.8 and $1.8\mu m$. Also, mould temperature needs to be controlled within certain range.

Projected area of runner on the parting surface should be minimal. The injection area actually is decreased if we decrease projected area, which diminishes the opening force of mould. In this way, we can adequately use the clamp force of injection machine to clamp the mould.

The smaller the runner volume is the better. This would improve utilization ratio of raw materials and save energy. The runner volume with fixed length would become smaller as the runner cross-section shape area decreases. Hence, the runner cross-section shape area should not be oversize.

Runners with advantages mentioned above can be considered to have high efficiency. And runner efficiency is expressed by equation 2.

$$\eta = \frac{S}{L \bullet l} \tag{2}$$

where η is runner efficiency, S is runner cross-section shape area, L is peripheral length of runner cross-section shape, l is runner length and $L \bullet l$ is runner lateral area.

Equation 2 illustrates that runner efficiency is equal to the ratio of runner cross-section shape area to its lateral area. Also, the runner lateral area is equal to the peripheral length of runner cross-section shape multiplied by runner length. Therefore, increasing the runner cross-section shape area, decreasing the peripheral length of runner cross-section shape and reducing the runner length all can improve runner efficiency. In this paper, runner efficiency refers to the runner efficiency when runner length is unit length ($l = 1$). Its value is equal to the ratio of runner cross-section shape area to its peripheral length (equation 3).

$$\eta = \frac{S}{L} \tag{3}$$

Runner efficiency is influenced by its cross-section shape area and peripheral length. Therefore, runner efficiency is related to its geometric parameters of cross-section shape.

We compare various runners under the same conditions (Table 3). In the Table 3, η is runner efficiency and D is runner width. Cross-section shape areas of different runners are the same ($s = 1mm^2$) when calculating η and D. V is the runner volume when runner length is unit length and efficiency is 1 ($\eta = 1$). According to Table 3, the width of rectangular runner is minimal. Dimension of runner projection on the parting surface would be decreased if we reduce the width, which improves the mode-locking of the injection

machine. This is the main advantage of rectangular runner. However, it is rather difficult to demould for rectangular runner without demoulding inclination. Therefore, we usually use gate with rectangular cross-section in practice.

Runners	Circular runner	Semicircular runner	Rectangular runner	Ladder runner	U-shape runner
Efficiency of the runner η	0.282	0.244	0.250	0.250	0.262
Width of the runner D	1.13	1.60	1.00	1.07	1.12
Volume of the runner with unit length V	12.57	16.83	16.00	16.04	14.61

Table 3. Comparison between the analytical solutions of various runners.

The efficiency of circular runner is highest and its runner volume to its unit length is minimal. Decreasing runner volume can promote the utilization of raw materials and save energy. However, if the circular runner is used in the cold-runner mould, circular runner needs to be divided into two semicircular runners on the parting surfaces of cover half and moving half respectively. These two semicircular runners have to be exactly the same. Therefore, it would be very difficult to manufacture mould with circular runners. Usually, the circular runners are used in the hot-runner mould rather than in the cool-runner mould.

Apparently, with the same cross-section shape area, efficiency of U-shape runner is highest compared with that of semicircular and ladder runners. The width of U-shape runner is smaller than that of circular runner. With the same efficiency and length (unit length), the volume of U-shape is minimal among the semicircular, ladder and U-shape runners and next to that of circular runner. Therefore, U-shape is most suitable in the cool-runner mould. Semicircular runner is not the perfect approach for its minimal efficiency and largest width and volume.

2.2 Modeling and mesh generation

Table 4 shows the parameters of various cross-section shapes with the same area ($S = 4\pi$).

Runners	Cross-section shapes	Parameters	Values (mm)
Circular	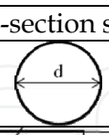	Diameter D ($2r$)	4
semicircular	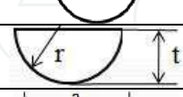	Diameter D ($2r$), height (t)	D=5.65; t=2.825
Rectangular	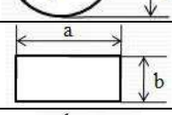	Width (a), height (b)	a=b=3.54
Ladder	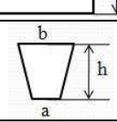	Upper line (b), lower line(a), height(h)	b=3.8; a=3.3; h=3.534
U-shape	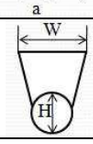	Width (W), height(H)	W=3.98; H=3.71

Table 4. Parameters of various cross-section shapes.

2.3 Feedstock rheology

Compositions of ZrO_2 feedstock are filler (solid paraffin), adhesive (vinyl acetate polymer) and lubricant (stearic acid). These compositions are shown as Table 5 (Wenjea et al., 1999) and the relationship between viscosity and shear rate is shown as Fig. 3.

	Zirconia (PSZ)	stearic acid (SA)	solid paraffin(PW)	Vinyl acetate polymer
Mass fraction (%)	86.7	0.9	7.0	5.4
Volume fraction (%)	50.0	3.3	28.0	18.7

Table 5. Compositions of ZrO_2 feedstock.

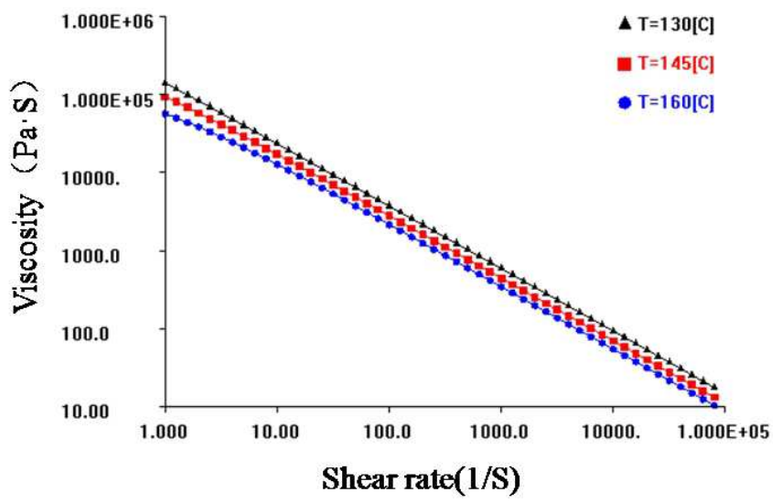

Fig. 3. Relationship between viscosity and shear rate.

2.4 Simulation outcomes

Pressure drop, filling time, temperature difference and clamp force determines the product quality and these are important parameters of injection machine. In this paper, we use the parameters mentioned above to discuss simulation outcomes of various cross-section shapes (Fig. 4, Fig. 5, Fig. 6, Fig. 7).

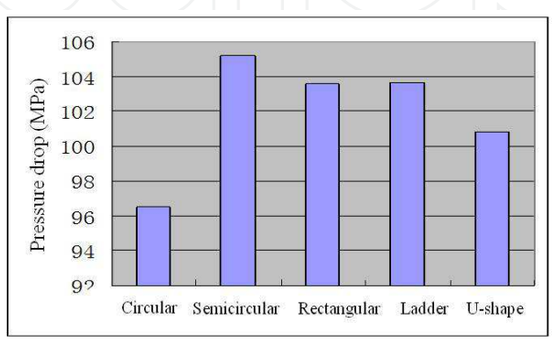

Fig. 4. Pressure drop simulation.

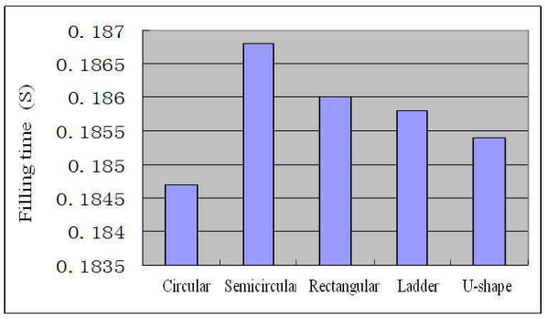

Fig. 5. Filling time simulation.

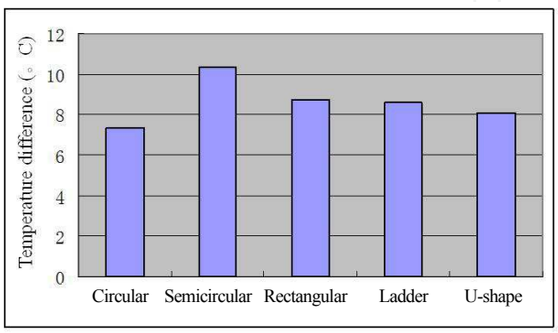

Fig. 6. Temperature difference simulation.

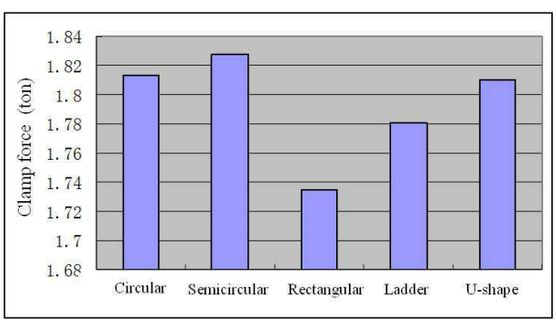

Fig. 7. Clamp force simulation.

During these simulations, injection temperature is 140° C and mould temperature is 60° C. Injection time, pressure and velocity are controlled by program. The simulation outcomes of various runner cross-section shapes are shown as Table 6.

Serial number	Cross-section shape	Pressure drop (MPa)	Filling time (s)	Temperature difference (°C)	Clamp force (ton)
A	Circular	96.492	0.1847	7.3	1.8128
B	Semicircular	105.177	0.1868	10.3	1.8277
C	Rectangular	103.587	0.1860	8.7	1.7344
D	Ladder	103.668	0.1858	8.6	1.7811
E	U-shape	100.792	0.1854	8.1	1.8101

Table 6. Analytical parameters of various runner cross-section shapes.

Injection pressure is an important, technical parameter of injection molding. It should not be too high or it may be hard to demould and cause raw edges on the product surface. What is more, the melt would not be able to fully fill mould cavity if the injection pressure is too high. Therefore, a suitable injection pressure is very necessary. Improving the injection pressure can improve the melt compression ratio and dimension accuracy (Liu et al., 2002). Runners with different cross-section shapes are compared under the same conditions (Table 7).

Runner	Circular	Semicircular	Rectangular	Ladder	U-shape
Cross-section shape	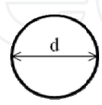	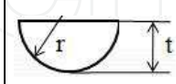	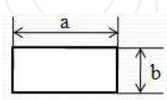	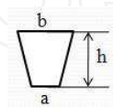	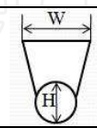
Pressure drop ranking	1	5	3	4	2
Filling time ranking	1	5	4	3	2
Temperature difference ranking	1	5	4	3	2
Clamp force ranking	4	5	1	2	3
Processability	Hard	Easy	Easy	Easy	Easy
Removing the cold material	Easy	Easy	Hard	Easy	Easy
Comprehensive evaluation	Suitable	Unsuitable	Rarely use in practice	Perfect	Most suitable for cold runner

Table 7. Comparison between runners.

According to Table 7, circular runner has minimal pressure drop, shortest filling time and smallest temperature difference, which means that it has the highest efficiency. On the other hand, rectangular runner has the smallest clamp force.

Compared with semicircular and ladder runners, U-shape runner has smallest pressure drop, shortest filling time, minimal temperature difference and highest efficiency. Therefore, runner with U-shape cross-section shape is the best choice.

3. Layout of runner system and optimization of technical parameters

During Ceramic Injection Molding stage, raw materials within staff canister firstly are heated to become melt which is driven quickly by the piston or screw into the closed cavity. Then, the melt within mould cavity compressed by mould and cools down to become product. The main concern of Ceramic Injection Molding is that the products should meet the quality requirement. Also, the solid load of ceramic powder, which is related to the product quality, should be as high as possible.

The conventional methodology optimizing process parameters requires experts use the trial and error method basing on their experience and professional knowledge. As the development of CAE technology, it becomes increasingly important to industry, especially to improve product quality and decrease cost etc. We combine CAE experiment and DOE

methodology to get the best parameter combination based on the range analysis of orthogonal experiment. Also, the conclusion could be tested by the CAE comparison experiments.

3.1 Layout of runner system

The mould is composed of two templates with six cavities and common arrangement of multi-cavity system is radiated runner system. Melt can only be poured into the cavity through gates on both sides of mould for there is a fairly small hole in the axial center of products. Runner systems with rectangular and circular shunt are showed as Fig. 8 (Zhang, 2005, 2007).

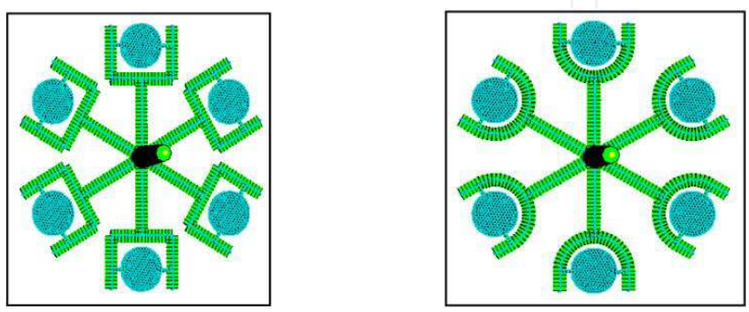

(a) (b)

Fig. 8. Two runner systems; (a) Runner system with rectangular shunt; (b) Runner system with circular shunt.

3.2 Orthogonal experiment methodology

Injection molding CAE technology uses finite element methodology, finite difference methodology and boundary element methodology to analyze the flow, dwell and cooling stage. It can calculate stress distribution within product and mould to predict product quality. Also, it can analyze the influences of process conditions, material parameters and mould structure on the products for the purpose of optimizing mould structure and process parameters.

Experiment design method (DOE) is mainly used to acquire the experimental data and analyze the experimental data and results scientifically. The main DOE application is the orthogonal experiment which designs the experiment based on data orthogonality (Yang et al., 2004). There are many distinct advantages of orthogonal experiment. Firstly, it can select a small number of experimental conditions, which are representative, from a large number of experimental conditions. Secondly, the best experimental conditions and manufacture process could be determined by analyzing experimental outcomes with those representative conditions. Finally, it would be much easier to process the data based on the orthogonal experiment.

Orthogonal table is the most important, basic tool and orthogonal experiments can easily calculate the effect of each condition on the results and display them by tables. Then, we can determine the best parameters after range analysis and comparison. All the calculations are done by tables and the whole processes are rather easy. Therefore, DOE is able to shorten the cycle of developing and designing new products, which is necessary to the manufacture and

research. During injection molding, injection process parameters directly affect the product quality. Many researchers have designed experiments to research the relationship between them and got some useful conclusions (Skourlis et al., 1997; Jansen et al., 1998). However, conventional methodology requires a large number of experiments to research that relationship. Yet, research demonstrates that an economic method is to use the orthogonal experiment which in turn can instruct the injection molding process (Jin & Zhu., 2000).

3.3 Arrangement of orthogonal experiment

In this paper, we focus on these two runner systems mentioned above and use orthogonal experiment method to study the influence of two runner systems on products.

Mould temperature, injection temperature, screw velocity and gate dimension all are important parameters influencing product quality. Mould temperature A, injection temperature B, screw velocity C and gate dimension D all have three different values, namely A1, A2, A3, B1, B2, B3, C1,C2, C3, D1, D2, D3. We use L9 (3^4) orthogonal table to design experiments and use Moldflow software to investigate the influence of those parameters on product quality.

	factor	Level 1	Level 2	Level 3
A	Temperature of mould (°C)	35/40	45/50	60/65
B	Injection temperature(°C)	130/135	145/150	160/165
C	Screw velocity (%)	75	60	50
D	Width and length of the gates（mm）	1, 0.5	1.2, 0.6	1.5, 0.8

Table 8. Arrangement of factors and levels.

Finally, we can obtain the best parameter combination. Values of four parameters mentioned are shown as Table 8 and orthogonal table L9 is shown as Table 9. We consider the actual filling time, maximal injection pressure and temperature difference at the end of filling stage as the main parameters. By orthogonal experiment, we can know that when we just consider one condition with different values, this condition would have much more effect on the result if it has a larger range (Shen et al., 2001, 2002). In order to demonstrate the influence of each condition on the injection flow, we draw the relation graphs between them as Fig. 9, Fig. 10 and Fig. 11 (Zhang, 2005, 2007).

Experimental number	A	B	C	D
1	1	1	1	1
2	1	2	2	2
3	1	3	3	3
4	2	1	2	3
5	2	2	3	1
6	2	3	1	2
7	3	1	3	2
8	3	2	1	3
9	3	3	2	1

Table 9. Orthogonal table.

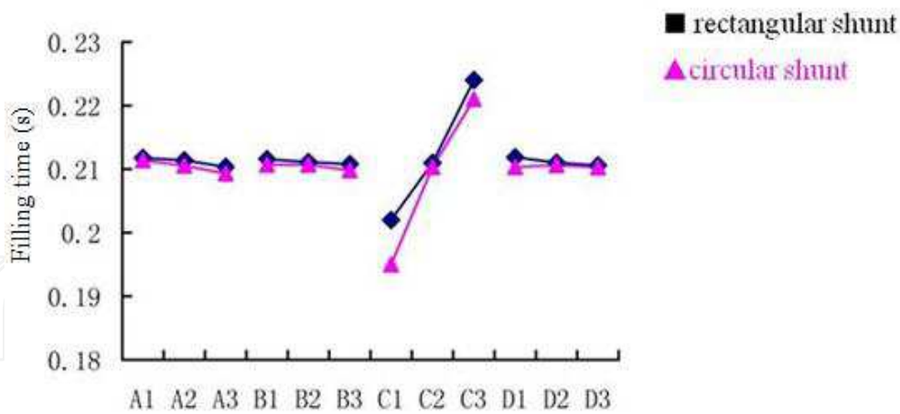

Fig. 9. Relationships between filling time and each factor.

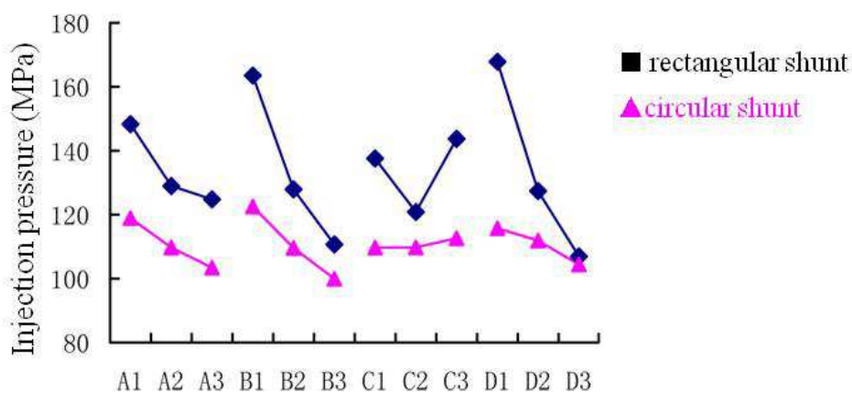

Fig. 10. Relationship between injection pressure and each factor.

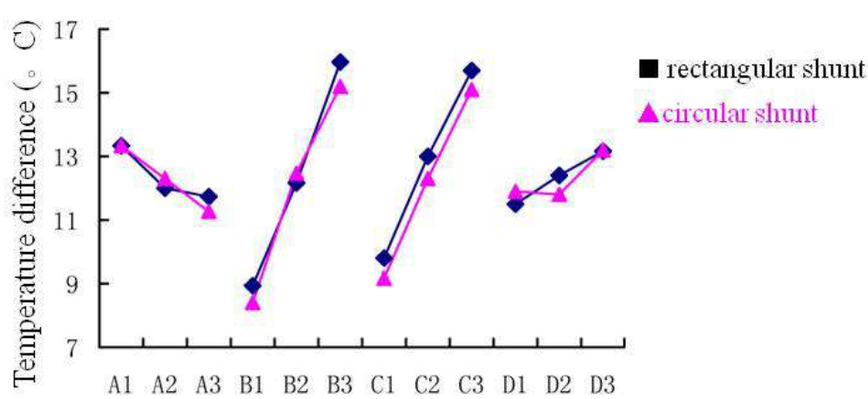

Fig. 11. Relationship between temperature difference and each factor.

3.4 Simulation results

Fig. 9 illustrates that screw velocity has largest influence on filling time. Therefore, increasing screw velocity can shorten filling time. Other factors influence filling time slightly.

Product quality could be improved by decreasing injection pressure. According to Fig. 10, we can see that injection temperature and gate dimension have largest effect on injection pressure. Therefore, improving injection temperature could decrease the injection pressure. Also, gates with too small dimension require comparatively large injection pressure.

Comparatively small temperature difference could be beneficial to the homogenous filling of powder and adhesive, which can prevent temperature gradient and density gradient caused by two-phase separation. Fig. 11 demonstrates that injection temperature and screw velocity have largest effect on temperature difference and next is the gate dimension and mould temperature. Hence, lower injection temperature and higher screw velocity contribute to decrease product surface temperature difference.

	Injection time (s)	Injection pressure(MPa)	Temperature difference (°C)
Rectangular shunt	0.195	108	9.1
Circular shunt	0.182	95.1	6.9

Table 10. Simulation outcomes of best parameter combination.

Considering all the factors, we can conclude that the best parameter combination of runner system with rectangular shunt is A2B2C2D3 and best parameter combination of runner system with circular shunt is A3B2C1D2. Simulation outcomes of two runner system are shown as Table 10. What is more, filling quality of runner system with circular shunt is much better than that of runner system with rectangular shunt and injection pressure the former runner system requires is 15MPa, less than that of the latter. Filling time and surface temperature difference of the former one are much smaller compared that of the latter one. Therefore, runner system with circular shunt is most suitable for ceramic injection molding.

4. Gravity influence on the ceramic injection mould

The melt fills five of six cavities well except the one on the top of mould where short shop happens. However, mould with six cavities is designed to have balance runner system, which means that the six cavities should all be filled well. Therefore, gravity should be taken into consideration for large runner length, zirconia density and viscosity.

In order to simplify the calculation and analysis, we select two cavities on the top and bottom parts of mould respectively as research objects. Fig. 12(a) demonstrates the simulation outcomes with conditions namely mould temperature (60°C), injection temperature (145°C), screw velocity (75%) and gate dimension (1.2mm and 0.6mm) when considering gravity influence. According to Fig. 12(a), we can see that cavities show difference in filling stage. Filling time of bottom die is much less than that of top die where the short shot happens. Also, bottom die quality is better than that of top die (Zhang, 2005, 2007).

4.1 Improvement

Two cavities on the top and bottom parts of mould show difference on the filling stage and short shot happens on the top cavity. Therefore, we increase runner diameter from 4mm to 4.17 mm. Fig. 12(b) illustrates that both the top and bottom dies with optimized balance runner system have same quality.

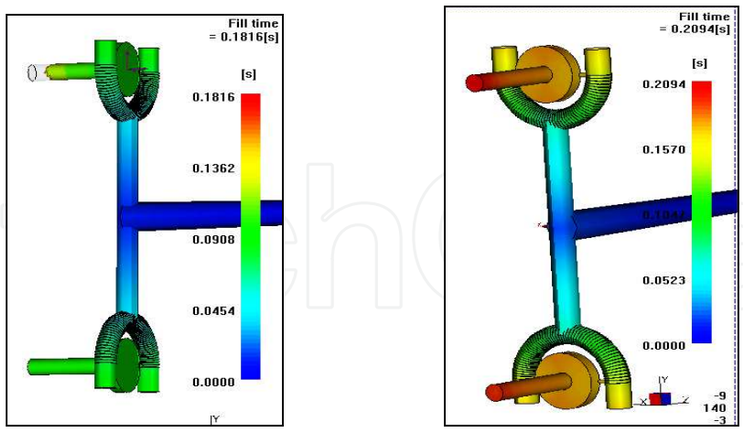

(a) (b)

Fig. 12. Simulation of gravity effect on ceramic injection molding; (a) runner diameter is 4mm; (b) runner diameter is 4.17mm.

5. Cooling simulations

Injection molding cooling refers to the stage after solidification to demould products from mould which occupies 3/4 of product cycle. Cavity temperature and uniformity directly influences product efficiency and quality. Injection molding temperature can be affected by various factors. Temperature control and regulation are mainly accomplished by cooling system. Cooling process parameters are composed of cooling pipeline dimension, connection and location etc. Physical parameters include cooling medium flow and gate temperature etc. The most important process parameter during cooling stage is cooling time and an efficient and balance cooling system could improve cooling efficiency and decrease residual stress. The purpose of cooling analysis is to determine cooling system though simulating the cooling process which predicts the surface temperature of mould and cooling time etc.

5.1 Summary of cooling simulation

The main stages of injection molding cycle are filling, dwell and cooling stages. The heat transfer process of injection molding shows that inner part of melt with high temperature transfers heat to the mould and the heat is taken by cooling medium. Therefore, balance cooling could prevent hot streak on product surface and decrease warpage and residual stress within product.

Injection molding cooling is mainly controlled and regulated by cooling system. The main purpose of cooling system is to cool the product fast and evenly. Cooling system parameters are composed of geometric and process parameters like cooling hole location, dimension, cooling medium flow and gate temperature. Cooling stage simulation could predict the cavity and core temperature, temperature difference distribution and cooling time with given parameters (Chen et al., 2002).

5.2 Establishing the mathematical model

5.2.1 Basic assumption and controlling equation

Physical process of cooling stage is fairly complex and we need simplify physical process before constructing controlling equation. Firstly, we assume that the mould work state is stable without considering periodic temperature changes of die well. Secondly, we assume that the heat flow only propagates along the normal direction of inner cavity surface. Thirdly, we assume that the product surfaces and die well have the same temperature and the product contacts cavity surface completely.

Based on the assumption mentioned above, we consider the injection molding cooling to be steady heat conduction without heat source. And controlling equation is equation 4(Li et al., 2001).

$$\frac{\partial^2 T}{\partial x^2}+\frac{\partial^2 T}{\partial y^2}+\frac{\partial^2 T}{\partial z^2}=0 \quad (x,y,z)\in V \tag{4}$$

Where V is the region enclosed by outer surface of mould, inner surface of cavity and surface of cooling gates.

5.2.2 Boundary conditions

Boundary condition on the cavity surface is equation 5 (Li et al., 2001).

$$-K_w\frac{\partial T}{\partial u}=\bar{q} \tag{5}$$

where u is out normal direction of cavity surface, K_w is thermal conductivity of mould and $\bar{q}$ is average heat flux which is defined by equation 6.

$$\bar{q}=\frac{1}{t_c+t_p}\left\{\int_0^{t_c} q_1(t)dt+\int_0^{t_c+t_p} q_2(t)dt\right\} \tag{6}$$

where t_c and t_p are cooling and demoulding time respectively, $q_1(t)$ and $q_2(t)$ are the instantaneous heat flux during cooling and demoulding stage. The cooling time t_c and $q_2(t)$ could be obtained by solving the one dimension transient heat conduction equation (equation 7).

$$\rho C_p\frac{\partial T}{\partial t}=\frac{\partial}{\partial s}(K_p\frac{\partial T}{\partial s}) \tag{7}$$

where t is the time, T is the melt temperature, ρ, K_p and C_p are the density, heat conductivity and equivalent specific heat respectively and s is local coordinate along the product thickness direction. When analyzing one dimension transient heat conduction of injection mould, we consider the injection temperature or melt temperature distribution at the end of filling stage to be the initial condition. Also, we select the cavity surface temperature as the boundary condition.

The boundary condition of gate surface is defined as equation 8 (Li et al., 2001).

$$-K_m \frac{\partial T}{\partial u} = h(T - T_c) \tag{8}$$

where u is outer normal direction of gate surface, T_c is cooling medium temperature, h is heat transfer coefficient between mould and coolant (equation 9).

$$h = 0.23 \frac{kc}{D} R_e^{0.8} P_r^{0.4} \tag{9}$$

Where $R_e = 4Q / \pi D\nu$ is Reynolds number, $P_r = \nu / a$ is Prandtl number, Q is the coolant volume, D is the cooling hole diameter, ν , a and kc are the kinematic viscosity, thermal diffusivity and heat conductivity respectively.

The outer surface heat exchange of mould normally does not have much effect on the temperature distribution of cavity surface, which means that it is unnecessary to calculate outer surface temperature distribution of mould. Therefore, we can consider the outer surface of mould to be an infinite, adiabatic sphere.

5.3 Cooling analysis and moldflow software application

Regulating and keeping the mould temperature could decrease product deformation and improve mechanical properties and dimension accuracy. Therefore, it is necessary to design the cooling system perfectly for injection molding. Researchers have done a lot of research related to the cooling system and got many simplified and empirical formula. MPI/Cool can analyze the effect of cooling system on the mould and optimize arrangement of cooling system.

5.3.1 Summary of MPI/cool software

Many factors affecting the injection molding cooling are product shape, cooling medium type, temperature, velocity, geometric parameters and arrangement of cooling pipe, mould material, melt temperature, ejected temperature, mould temperature and thermal cycling interaction between production and mould etc. These factors interact and relate with each other, which means that the best methodology is to combine these parameters. Yet, it only can be achieved by CAE analysis rather than by conventional simplified and empirical formula.

MPI/Cool software simulates this three dimension temperature field by boundary element method. Analytical solution could be used to calculate temperature field along the product thickness direction. What is more, MPI/Cool can obtain the interactive solution between mould temperature field and temperature field along the product thickness direction. Also, MPI/Cool can calculate the interface temperature between product and mould by the simultaneous energy equation of mould temperature field. Furthermore, we consider the influence of cavity and core asymmetry along the thickness direction on the product temperature distribution.

MPI/Cool can simulate the cooling pipe (separator pipe, jet pipe and connecting hose), insert, various mould materials, cool runner and hot runner, parting surface and product temperature. This can provide information for optimizing the cooling system.

MPI/Cool can not only analyze the neutral plane and fusion mould but also analyze 3D mould. Also, the dynamic analysis of injection process could be obtained by combining MPI/Cool and MPI/Flow.

5.4 Cooling simulation

Product mould could be constructed by Pro/E and UG etc. which can be read into MPI by STL file format. Then, cooling system and gating system are built in MPI. Three different cooling systems are shown Table 11 (Liu et al., 2010).

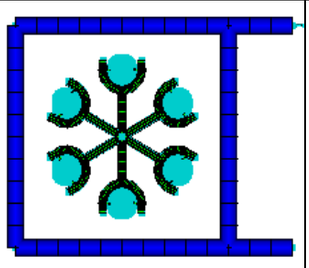	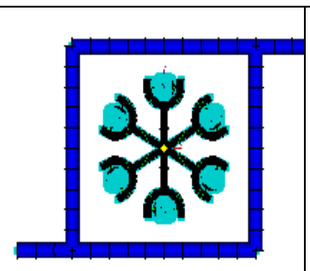	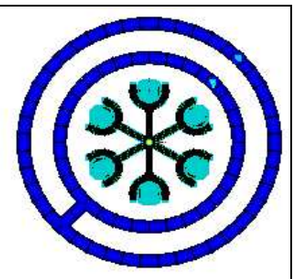
Cooling system one	Cooling system two	Cooling system three

Table 11. Arrangement of cooling systems.

5.4.1 Input the process parameters

We set the melt temperature, cavity temperature and cooling pipe diameter to be 150°C, 40°C and 8mm respectively. The coolant is water (25°C) and Reynolds number is 10000. Finally, we use t software to calculate cooling time.

5.4.2 Simulation results of cooling time

We obtain coolant temperature, coolant velocity, cooling pipe temperature and Reynolds number of coolant (Fig. 13, Fig. 14, Fig. 15) after analyzing cooling process.

According to Fig. 13, Fig. 14, Fig. 15, we find that pipe and coolant temperature distribution in the third cooling system is much more homogeneous than that in the former two. In order to compare the cooling efficiency of three different cooling systems, we can calculate the cooling time of three cooling system by software. The calculated cooling time is shown as Table. 12. According to Table. 12, the first cooling system has longest cooling system, next is the second cooling system and the third cooling system has shortest cooling time.

Therefore, the third cooling system has best heat balance and cooling efficiency.

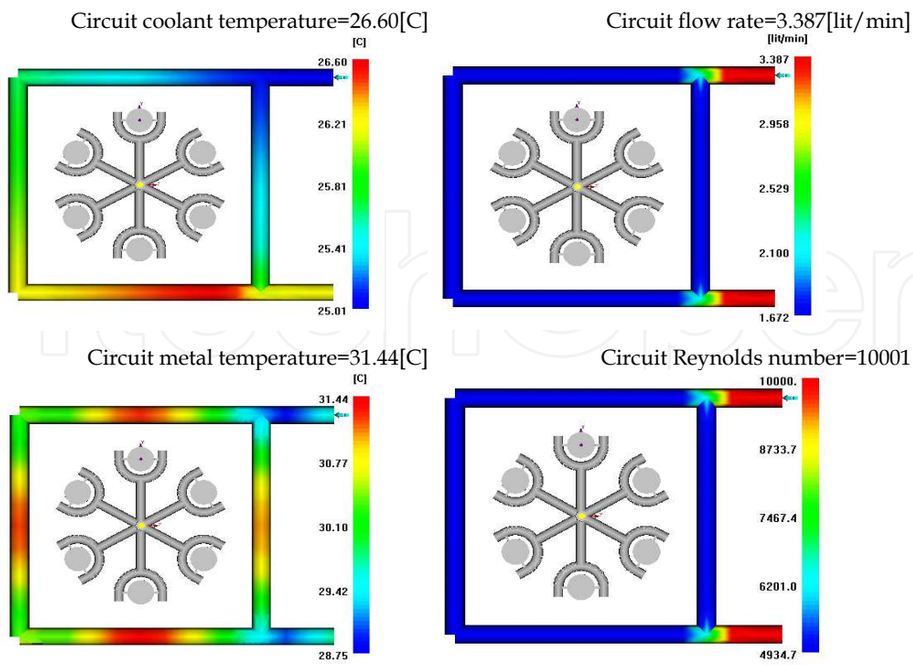

Fig. 13. Simulation outcomes of first cooling system.

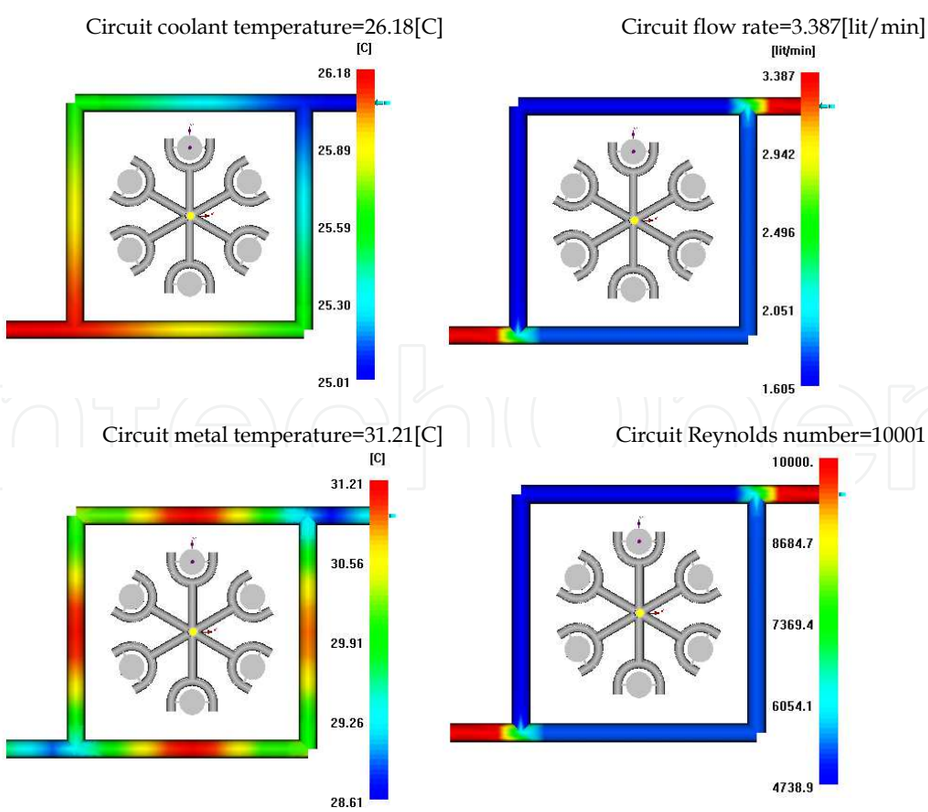

Fig. 14. Simulation outcomes of second cooling system.

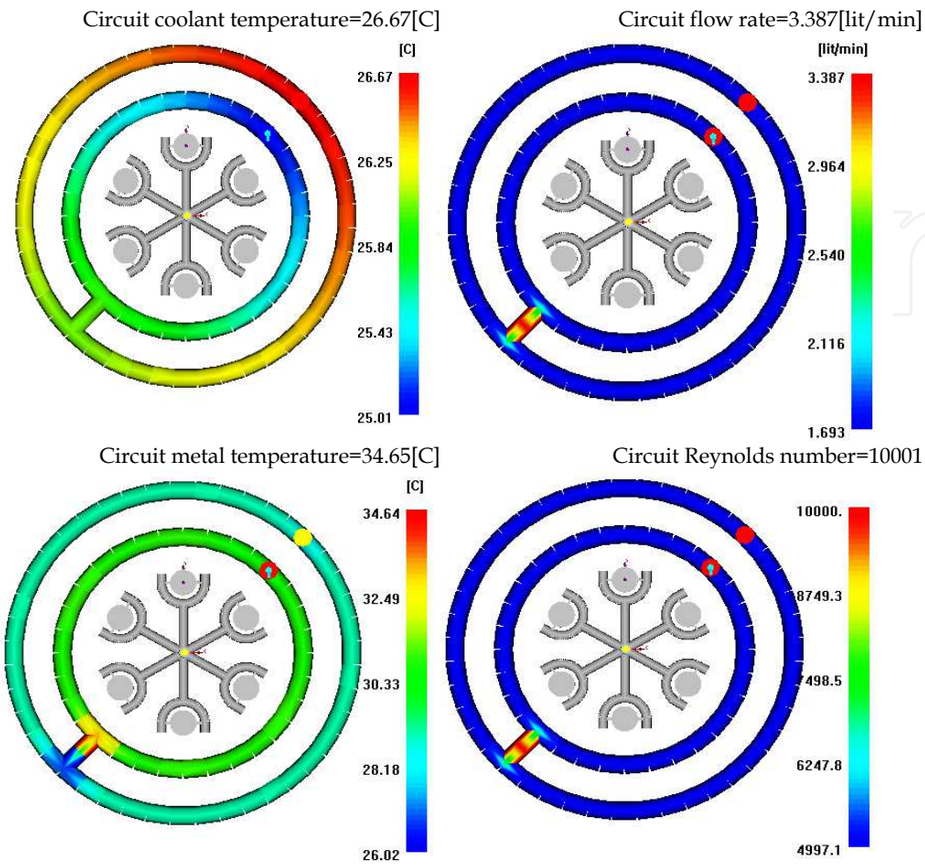

Fig. 15. Simulation outcomes of third cooling system.

	Cooling system one	Cooling system second	Cooling system three
Cycle time (S)	38.9850	37.9800	32.5205

Table 12. Cycle time of different cooling system.

5.5 Comparison between simulation results of these three cooling system

There are two kinds of cooling analysis, namely manual and automatic cooling analysis. We need to set the cooling time when using manual cooling analysis. Cooling time is calculated by software in the automatic cooling analysis. We use the automatic approach to analyze the cooling efficiency of three different cooling systems in the former chapter. In order to compare their cooling efficiency with given cooling time, we use the manual cooling analysis and set the cycle period to be 35s, 30s, 25s respectively.

During cooling process, six cavities are cooled unevenly for the different arrangement of cooling pipes. We number the six cavities according to clockwise direction (Fig. 16 (a)) and select the top, middle and bottom parts of every cavity (Fig. 16(b)) to analyze the temperature distribution of each cavity with different cooling condition.

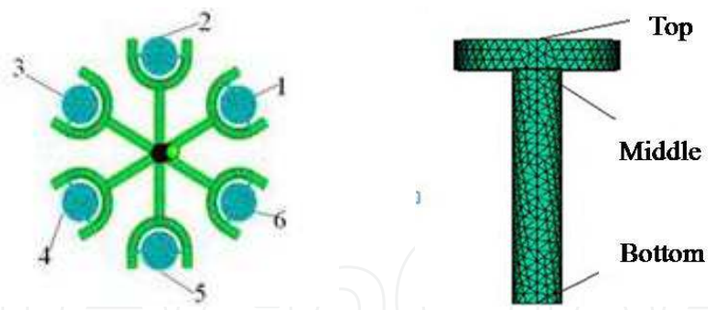

(a) (b)

Fig. 16. Cavity labels; (a) Number of cavities; (b) Three locations in each cavity.

5.5.1 Simulation outcomes with 35s cycle period

Table 13 demonstrates the general temperature difference of product in three cooling systems respectively when cycle period is 35s. According to Table 13, product temperature difference in the first cooling system is similar to that in the second cooling system. Also, temperature difference in the third cooling system is comparatively higher for it cools much faster, which causes local parts cool significantly. However, product temperature differences in these cooling systems all are acceptable.

	Maximum temperature	Minimal temperature	Temperature difference
Cooling system one	46.13	37.34	8.79
Cooling system two	45.93	37.15	8.78
Cooling system three	45.19	36.35	8.84

Table 13. General temperature difference of product when cycle period is 35s (°C).

Table 14 illustrates the temperature simulation of three different parts in the cavity axis in different cooling systems when the cycle period is 35s. According to Table 14, the given part temperature in certain cavity in the first cooling system is the highest. Next is the second cooling system. The given part temperature in certain cavity in the third cooling system is the lowest.

Number of cavities		1	2	3	4	5	6	Maximal difference
Cooling system one	Top	41.90	41.94	41.97	41.98	41.96	41.92	0.09
	Middle	46.10	46.19	46.21	46.26	46.25	46.15	0.16
	Bottom	37.74	37.80	37.9	37.91	37.89	37.85	0.17
Cooling system two	Top	41.68	41.68	41.75	41.70	41.72	41.76	0.08
	Middle	45.53	45.55	45.66	45.60	45.59	45.58	0.13
	Bottom	37.53	37.54	37.65	37.68	37.60	37.68	0.15
Cooling System three	Top	40.99	41.01	41.05	41.03	41.03	41.04	0.06
	Middle	44.69	44.71	44.79	44.75	44.80	44.74	0.11
	Bottom	36.67	36.70	36.75	36.73	36.75	36.76	0.09

Table 14. Temperature simulation of three different parts in the cavity axis in different cooling systems when cycle period is 35s (°C).

The cooling effect of given position varies in different cavities. In the first cooling system, Cavity one and two near the coolant inlet have better cooling effect compared with cavity three and four. In the second cooling system, cavity one and six have better cooling effect compared with cavity four and five. In the third cooling system, Cavity one has the lowest temperature. However, the general temperature of six cavities is approximately the same.

In these cooling systems, the extreme value of temperature difference of each cavity is shown as Fig. 17. It demonstrates that the extreme value of temperature difference of top, middle and bottom parts in the third cooling system is much lower than that in the former two, which means that the third cooling system has the best cooling efficiency.

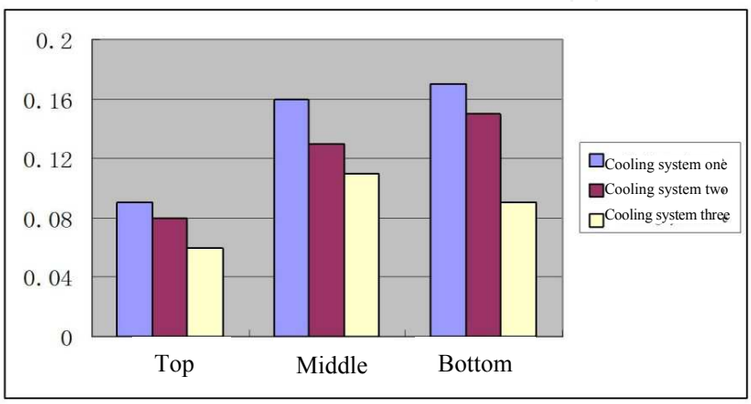

Fig. 17. Extreme values of temperature difference of various positions in each cavity when cycle period is 35s (°C).

5.5.2 Simulation result with 30s cycle period

Table 15 demonstrates the general temperature difference of product in these three cooling systems when the cycle period is 30s.

According to Table 15, product temperature difference in the first cooling system is similar to that in the second cooling system. On the other hand, product temperature in the third cooling system is comparatively higher. Therefore, simulation results are similar to that in three cooling systems when the cycle period is 35s.

	Maximum temperature	Minimal temperature	Temperature difference
Cooling system one	48.84	38.98	9.86
Cooling system two	48.62	38.76	9.86
Cooling system three	47.80	37.87	9.93

Table 15. General temperature difference of products when cycle period is 30s (°C).

Table 16 illustrates temperature simulation outcomes of three different positions in six cavities in three cooling system when the cycle period is 30s. In the first cooling system, cooling effect of given position in product varies in different cavities. Cavity one and six near the water inlet have better cooling efficiency. Next is cavity two and five. Positions in

cavity three and four have comparatively high temperature. Cavity three and four do not have ideal cooling efficiency. In the second cooling system, product temperature in the cavity one and six is much lower than that in the cavity three and five. In the third cooling system, cavity one and six have much lower temperature. However, temperature distribution in six cavities is even.

Number of cavities		1	2	3	4	5	6	Maximal difference
Cooling system one	Top	44.10	44.11	44.23	44.25	44.19	44.15	0.15
	Middle	48.15	48.19	48.37	48.36	48.28	18.20	0.22
	Bottom	39.49	39.50	39.52	39.69	39.62	39.56	0.20
Cooling system two	Top	43.95	43.98	44.09	44.03	44.05	44.08	0.14
	Middle	48.99	45.00	49.15	49.09	49.09	49.18	0.19
	Bottom	39.33	39.33	39.50	39.4	39.45	39.50	0.17
Cooling system three	Top	43.12	43.15	43.20	43.19	43.18	43.23	0.11
	Middle	47.32	47.34	47.49	47.41	47.43	47.45	0.17
	Bottom	38.38	38.41	38.51	38.46	38.49	38.55	0.16

Table 16. Temperature simulation outcomes of three different positions of six cavities in three cooling system when cycle period is 30s (°C).

Extreme values of temperature difference of various positions in each cavity when cycle period is 30s are shown as Fig. 18. The extreme values of temperature difference of top, middle and bottom part in each cavity in the third cooling system are smaller than that in the former two.

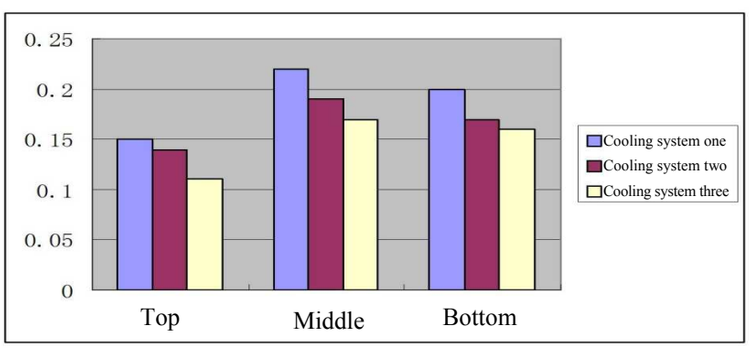

Fig. 18. Extreme values of temperature difference of various positions in each cavity when cycle period is 30s (°C).

5.5.3 Simulation outcomes when cycle period is 25s

Table 17 demonstrates the temperature difference of product with three cooling system when cycle period 25s. According to Table 17, temperature difference of product in the first cooling system is similar to that in the second cooling system. The general temperature difference of product in the third cooling system is the highest. Simulation results are similar to the outcomes obtained above.

	Maximal temperature	Minimal temperature	Temperature difference
Cooling system one	54.64	42.57	12.07
Cooling system two	54.37	42.30	12.07
Cooling system three	53.38	41.21	12.17

Table 17. General temperature difference of product when cycle period is 25s (°C).

Table 18 shows the temperature simulation of three different positions in different cooling system when the cycle period is 25s. Apparently, cooling efficiency of third cooling system is the best and temperature distribution of each cavity is even in the third cooling system.

Cavity Number		1	2	3	4	5	6	Maximal difference
Cooling system one	Top	49.10	49.08	49.27	49.31	49.19	48.17	0.23
	Middle	53.98	54.07	54.21	54.29	54.22	54.12	0.31
	Bottom	37.74	37.75	37.99	38.02	37.91	37.81	0.28
Cooling system Two	Top	48.83	48.85	48.99	48.92	49.02	48.91	0.19
	Middle	53.69	53.78	53.97	53.86	53.91	53.75	0.28
	Bottom	42.82	42.80	43.04	42.96	42.91	43.01	0.24
Cooling system three	Top	47.76	47.79	47.89	47.83	47.91	47.86	0.15
	Middle	52.78	52.83	52.99	52.89	52.90	52.93	0.21
	Bottom	41.88	41.90	42.07	41.98	42.01	42.03	0.19

Table 18. Temperature simulation of three different positions with different cooling system when cycle period is 25s (°C).

Extreme values of temperature difference of various positions in each cavity are shown as Fig. 19 when cycle period is 25s. The extreme values of temperature difference of top, middle and bottom parts in each cavity in the third cooling system are smaller than that in the former two.

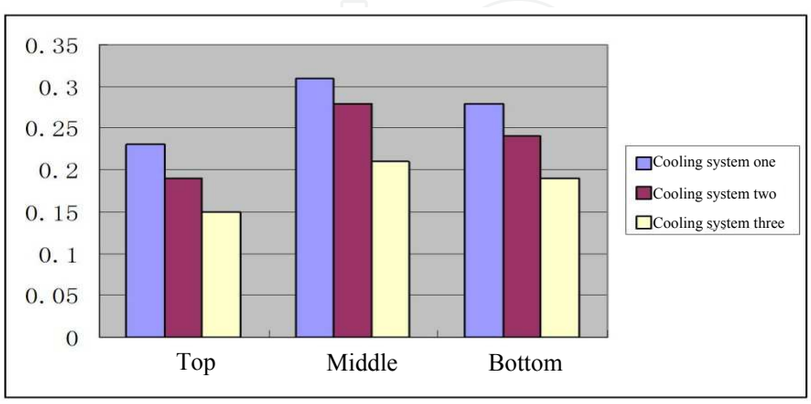

Fig. 19. Extreme values of temperature difference of various positions in each cavity when cycle period is 25s (°C).

6. Conclusion

Firstly, we used Moldflow to calculate pressure drop, filling time, temperature difference and clamp force of five different cross-section shapes. Outcomes demonstrate that U-shape runner has smallest pressure drop, shortest filling time, minimal temperature difference and highest efficiency. Therefore, U-shape runner is most suitable for cool-runner mould rather than circular or other kinds of runners.

Secondly, we investigated runner systems with rectangular and circular shunt respectively by orthogonal table. Also, we researched influence of mould temperature, injection temperature, screw velocity and gate dimension on products. Results show that runner system with circular shunt is most suitable for Ceramic Injection Molding. Furthermore, we considered the gravity influence on Ceramic Injection Molding and found that short shot tends to happen on the top cavity when runner diameter is 4mm. All six cavities are filled well after increasing runner diameter to 4.17 mm.

Finally, we simulated cooling efficiency of three cooling systems and results show that the third cooling system has shortest cooling cycle and best cooling efficiency, which can cool product as fast as possible. Cooling efficiency in six cavities is not the same for the cooling system arrangement and for the inlet and outlet location. Temperature extreme values of top, middle and bottom positions in each cavity in the third cooling system are smaller than that in former two cooling system.

7. References

Chen, J. B.; Shen, C. Y.; Wang, Z. F. (2002). Numerical simulation of the cooling process of Injection mould. *Polymer Materials Science & Engineering*, Vol.18, No. 4, pp.21-25, ISSN 1000-7555

Jansen, K. M. B.; Van, D. J.; Husselman, M. H. (1998). Effect of processing conditions on shrinkage in injection molding. *Polymer Engineering and Science*, Vol.38, No. 5, pp.838~846, ISSN 0032-3888

Jin, X. M.; Zhu, X. F. (2000). Investigating the influence of processing parameters of Injection Mould on the quality of the product by the orthogonal method. *Journal of south china university of technology*, Vol.28, No. 9, pp. 77-81, ISSN 1000-565X

Li, Q.; D, B. B.; Yang, M. S. et al. (2001). The Application of cooling simulation technology in the Injection mould and designing the processing parameters. *Engineering Plastics Application*, Vol.29, No. 4, pp.34-37, ISSN 1001-3539

Liu, F.; Lin, B.; Zhang, M. M.; Li, L. J. (2010). Redesign and optimization for ceramic injection mould of ZrO_2 fiber ferrule. Key Engineering Materials, Vol.434-435, pp.840-843, ISSN: 1662-9795

Liu, F. Q.; Yan, L. T.; Hu, H. Q. et al. (2002). Optimization of the refrigerator accouterment runner. *Engineering Plastics Application*, Vol.30, No. 4, pp. 39-42, ISSN 1001-3539

Pan, H. J.; Cui Q.; Pan, Y. J. (1995). Analysis of cross-section shape area of the runner of the Injection Mould. *China Plastics*, Vol.30, No. 4, pp. 79-87, ISSN 1001-9278

Shen, Y. K.; Yeh, P. H.; Wu, J. S. (2001). Numerical simulation for thin wall injection molding of fiber-reinforced thermoplastics. *International Communications in Heat and Mass Transfer*, Vol.28, No. 8, pp.1035~1042, ISSN 0735-1933

Shen, Y. K.; Liu, J. J.; Chang, C. T.; Chiu, C. Y. (2002). Comparison of the results for semisolid and plastic injection molding process. *International Communications in Heat and Mass Transfer*, Vol.29, No. 1, pp.97~105, ISSN 0735-1933

Skourlis, T. P.; Mohapatra, B.; Chassapi, C. et al. (1997). Evaluation of the processing parameters on the properties of advanced styrenic resins-A design of experiments approach. *Advances in Polymer Technology*, Vol.16, No. 2, pp.117-128, ISSN: 0730-6679

Wenjea J. T.; Liu, D.M.; Hsu, C.K. (1999). Influence of stearic acid on suspension structure and green microstructure of injection-molded zirconia ceramics. Ceramics International, Vol.25, No. 2, pp.191-195, ISSN 0272-8842

Yang, W.; Hu, S. G.; Jin, G. (2004). Optimal allocation of process parameters of Injection Mould based on the CAE, DOE and fuzzy weight. *Mechanical & Electrical Engineering Magazine*, Vol.21, No. 5, pp.37-40, ISSN 1001-4551

Zhang, M. M. (2005). Master Thesis, SME, Tianjin University, China

Zhang, M. M.; Lin, B. (2007). Simulation of ceramic injection molding for zirconia optical ferrule. Key Engineering Materials, Vol.336-338, pp.997-1000, ISSN: 1662-9795

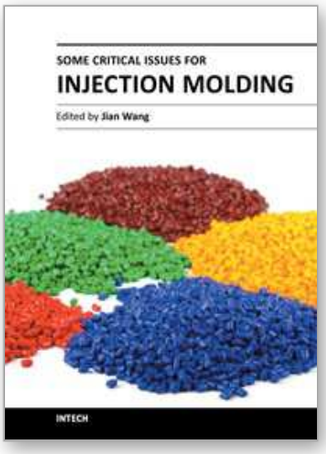

Some Critical Issues for Injection Molding

Edited by Dr. Jian Wang

ISBN 978-953-51-0297-7

Hard cover, 270 pages

Publisher InTech

Published online 23, March, 2012

Published in print edition March, 2012

This book is composed of different chapters which are related to the subject of injection molding and written by leading international academic experts in the field. It contains introduction on polymer PVT measurements and two main application areas of polymer PVT data in injection molding, optimization for injection molding process, Powder Injection Molding which comprises Ceramic Injection Molding and Metal Injection Molding, ans some special techniques or applications in injection molding. It provides some clear presentation of injection molding process and equipment to direct people in plastics manufacturing to solve problems and avoid costly errors. With useful, fundamental information for knowing and optimizing the injection molding operation, the readers could gain some working knowledge of the injection molding.

How to reference

In order to correctly reference this scholarly work, feel free to copy and paste the following:

Bin Lin, Meiming Zhang, Chuhan Wu and Feng Liu (2012). Optimization and Simulation for Ceramic Injection Mould of ZrO2 Fiber Ferrule, Some Critical Issues for Injection Molding, Dr. Jian Wang (Ed.), ISBN: 978-953-51-0297-7, InTech, Available from: http://www.intechopen.com/books/some-critical-issues-for-injection-molding/optimization-and-simulation-for-ceramic-injection-mould-of-zro2-fiber-ferrule

INTECH
open science | open minds

InTech Europe
University Campus STeP Ri
Slavka Krautzeka 83/A
51000 Rijeka, Croatia
Phone: +385 (51) 770 447
Fax: +385 (51) 686 166
www.intechopen.com

InTech China
Unit 405, Office Block, Hotel Equatorial Shanghai
No.65, Yan An Road (West), Shanghai, 200040, China
中国上海市延安西路65号上海国际贵都大饭店办公楼405单元
Phone: +86-21-62489820
Fax: +86-21-62489821

© 2012 The Author(s). Licensee IntechOpen. This is an open access article distributed under the terms of the Creative Commons Attribution 3.0 License, which permits unrestricted use, distribution, and reproduction in any medium, provided the original work is properly cited.